RSC Advances

ROYAL SOCIETY OF CHEMISTRY

www.rsc.org/advances

Electric field-dependent conductivity achieved for carbon nanotube-introduced ZnO matrix

Chunyu Shang,* Jinxian Zhao, Xiuqin Wang, Hongyang Xia and Hui Kang

In contrast to the carbon nanotube (CNT)-introduced insulating matrix, the electric conductivity of CNT-introduced ZnO matrix is not only dependent of the CNT content, but also dependent of the applied electric field when the CNT content approaches the electrical percolation threshold. In the view point of circuit interconnections in the microscope, there are two conductor-semiconductor contact structures equivalent to Schottky junctions being series connected between the adjacent CNTs, forming the electrical field-dependent impedances between the adjacent CNTs in the CNT-introduced ZnO matrix. Based on the electrical percolation theory, the CNT-introduced ZnO matrix may be seen to be a comprehensive circuit composed of a large amount of electrical field-dependent impedances being series and parallel connected. With the increasing of the applied electric field, these impedances would be decreased, leading to the inevitable decrease in resistivity of the CNT-introduced ZnO matrix. In essence, the electric field-dependent conductivity for CNT-introduced ZnO matrix is a macroscopic quantum tunneling effect. From a practical perspective in the electronics technologies, such a distinctive performance in electrical conductivity would have promising applications.

Department of Electronic and Information Engineering, Heilongjiang University of Science and Technology, Harbin 150027, P.R. China

*E-mail: shang.chun.yu@163.com.

1. Introduction

In the conventional composite conductive materials, the electrically conductive components, including metal powders, semiconductor powders and carbon derivatives of different morphologies, achieve the electrical conductivity in the insulating composite matrixes (polymers in general).[1-3] As indicated in the electrical percolation theory, with the amount of conductive component increases approaching the electrical percolation threshold, a three-dimensional conductive network begins to be formed in the composite matrix and the resistivity of composite conductive material decreases dramatically.[2, 4, 5] In contrast to the conventional conductive components, carbon nanotube (CNT) is distinctive due to its unique properties.[6-8] While the conductive characteristics of CNT-introduced insulating matrixes have no differences in contrast to those of conventional composite conductive materials except that a lower electrical percolation threshold is achieved.

In our research work, based on the electrical percolation theory of composite conductive materials and the related theories in solid state physics, multi-walled CNTs of a certain amount were introduced into Zinc oxide (ZnO, a typical semiconductor material) and the electric field-dependent conductivity for CNT-introduced ZnO matrix was identified to have been achieved. Meanwhile, the physical mechanisms in the distinctive performances have been theoretically investigated for the CNT-introduced ZnO matrix. From a practical perspective in the electronics technologies, the electric field-dependent conductivity for CNT-introduced ZnO matrix would have promising applications and our research work is of significant importance.

2. Experimental section

2.1 Preparation of material samples

Y_2O_3 sample was synthesized using the sol-gel method. 35 g of $Y(NO_3)_3 \cdot 6H_2O$ was dissolved in dilute nitric acid to form aqueous solution, then 170 g of citric acid ($C_6H_8O_7 \cdot H_2O$), 200 ml of glycol ($C_2H_6O_2$) and 10 g of polyethylene glycol ($HO(CH_2CH_2O)_nH$, molecular weight >20000) were added into the aqueous solution. The turbid suspension was stirred and

heated at 90 ºC for 5h to form a gel, the gel was preheated at 300 ºC for 2h and then sintered at 600 ºC for 2h to form Y_2O_3 sample in micrometer magnitude.

The micron-sized Y_2O_3 sample was attached with In_2O_3 by hydrolysis of indium isopropoxide ($In[OCH(CH_3)_2]_3$). Y_2O_3 sample, distilled water and isopropyl alcohol were added into the alkoxide solution of In. During churning of these reactants at 80ºC, hydrolysis and condensation occurred. After drying the solution and sintering at 600ºC for 8h, In_2O_3-introduced Y_2O_3 sample was formed.

In the preparation of multi-walled CNT-introduced Y_2O_3 sample, a certain amount of ethanol solution of multi-walled CNTs which had been sufficiently dispersed by powerful ultrasonic oscillation was added in the aqueous solution in the preparation of Y_2O_3 sample in the sol-gel method. The last sintering process was performed at 800ºC for 6h in a nitrogen atmosphere.

In the preparation of multi-walled CNT-introduced ZnO sample, 16.5 g of zinc acetate ($Zn(Ac)_2 \cdot H_2O$) was dissolved in 75 ml of deionized water to form aqueous solution, then 10 g of Ammonium citrate ($(NH_4)_3 C_6H_5O_7$) was added into the solution. The solution was heated to 70 ºC, and then 125 ml of ethanol solution of multi-walled CNTs which had been sufficiently dispersed by powerful ultrasonic oscillation was added in the solution under stirring and heating. After 2h, a certain amount of peptizing agent ($NH_3 \cdot H_2O$) was added, and $Zn(OH)_2$ gel was formed after a long time. After drying the gel and sintered at 800ºC for 5h in a nitrogen atmosphere, multi-walled CNT-introduced ZnO sample was formed.

The adopted multi-walled CNTs have diameters of ~8nm and lengths of 10-30 μm, with an electrical conductivity of ~1.5×10^4 s/m and a specific surface area of ~500 m^2/g.

2.2 XRD characterization and resistivity measurements

The crystalline phase of multi-walled CNT-introduced ZnO samples were identified by Rigaku-D/max 2500 X-ray diffractometer using Cu Ka radiation (λ= 0.15405 nm).

In the resistivity measurements, each of the sample was made into a cylindrical with diameter $2r$ = 13mm and thickness d = 2mm under a pressure of 1.5×10^2 Mpa. Electrodes were made by Al deposition on both sides of each sample. The resistance was measured by a 769YP-24B megohmmeter and the resistivity was calculated by the following formula,

$$\rho = \frac{\pi \cdot r^2 \cdot R}{d}$$

3. Results and discussion

3.1. General features for the conventional composite conductive materials

According to the electrical percolation theory of composite conductive materials, a suitable conductive filler, as a separate component, may be introduced to improve the conductivity of the composite matrix. In the experiment, Yttrium Oxide (Y_2O_3) was adopted as the typical composite matrix of a high resistivity, and Indium oxide (In_2O_3) was adopted as the conventional conductive component owing to its favorable compatibility in the preparation of composite conductive materials with inorganic matrixes.[9] The experiment indicated that the resistivity of In_2O_3-introduced Y_2O_3 matrix decreases gradually with the increasing of In_2O_3 content when the In_2O_3 content is relatively lower, and decreases dramatically above the electrical percolation threshold P_{th} (P_{th} ≈25wt.% for In_2O_3-introduced Y_2O_3 matrix), and then decreases slightly with further increasing of In_2O_3 content, as shown in Fig. 1. The characteristics in resistivity-conductive content relation for In_2O_3-introduced Y_2O_3 matrix is typical for the conventional composite conductive materials.[9, 10] The electrical percolation theory indicates that when the conductive content increases to the electrical percolation threshold, a three-dimensional conductive network begins to be formed in the matrix.[10-13] As for the formation of conductive network, the dominant mechanisms lie in the physical contacts between the conductive fillers. Meanwhile, the quantum tunneling effect would play a role in the formation of conductive network, especially when the size of conductive component is in nanometer magnitude.[10] For a certain composite conductive material, the electrical percolation threshold P_{th} is nearly independent of the composite matrix and largely determined by the parameters such as conductivity, size and morphology of the conductive component.[10]

3.2. Low electrical percolation threshold and weak tunneling effect in the CNT-introduced insulating matrix

In contrast to the conventional conductive components, CNT is distinctive due to its unique properties. Consequently, distinctive performances may be expected for CNT-introduced composite materials. CNTs are rolled graphite sheets with diameters in nanometer magnitude and lengths in micrometer magnitude, possessing one-dimensional morphorlogy of rather larger aspect ratios. CNTs can be classified to be single-walled CNTs and multi-walled CNTs, possessing remarkable mechanical strength, reliable chemical stability, high melting point and excellent electrical conductivity.[6-8] In contrast to the single layer structure of single-walled CNTs, the structure of multi-walled CNTs is cylinders inside cylinders. The resistivity-conductive content relation for multi-walled CNT-introduced Y_2O_3 matrix is similar to those of conventional composite conductive materials, as shown in Fig. 2. While the electric percolation threshold, i.e., the CNT content at which the three-dimensional conductive network begins to be formed in the composite matrix, is rather low (P_{th} ≈1.5wt.% in the experiment), to be at least an order of magnitude lower than the conventional conductive components. In theory, the electric percolation threshold of CNTs in the composite matrix may be further lower, as reported in literatures.[3, 14, 15] The low electric percolation threshold of CNTs is originated in the unique structure and excellent conductivity of CNTs (>150 s/cm). The one-dimensional morphology of CNTs with large aspect ratios (>1000) would make them an excellent conductive component in the composite matrix. Although the directions of CNTs would be distributed randomly in the matrix, each of them has a component parallel to the applied electric field. Consequently, in the view point of charge transmission, the one-dimensional morphology of CNTs is apparently a merit.[16-18] As an excellent conductive component, multi-walled CNTs are more suitable to be introduced into the composite matrix than the single-walled CNTs. The reason lies in the fact that if the electric conductivity of the outer layer of a multi-walled CNT is deteriorated in the combination with the composite matrixes owing to the ultra-large specific surface area of the CNT (>500 m^2/g), the inner layer would conduct independently, ensuring the conductive function of the CNT.

As has been pointed out in literatures, the quantum tunneling effect may play a role in the formation of conductive network when the size of conductive component is in nanometer

magnitude.[10] In principle, for a certain conductive component and a certain composite matrix, the tunneling effect would be apparent when the average distance of adjacent conductive fillers is decreased and the applied electric field is increased in the composite conductive material. Meanwhile, the tunneling currents between the adjacent conductive fillers would increase super-linearly with the increasing of the applied electric field, leading to the current nonlinearity in the composite conductive material. However, in the experiments, the electric field-current relation for multi-walled CNT-introduced Y_2O_3 matrix has been identified to be linear. The electric field-current linear relation is different for different CNT contents, corresponding to different resistivity of multi-walled CNT-introduced Y_2O_3 matrix. The linearity in the electric field-current relation indicates the tunneling effect is negligibly weak, and the physical contacts between the conductive fillers should be the dominant mechanisms in the formation of conductive network. In principle, the weak tunneling effect, which is independent of CNT content in CNT-introduced Y_2O_3 matrix, is originated in the high potential barriers between the CNTs and the insulating matrix, and the height of the potential barriers should be able to be adjusted by the application of different composite matrixes.[19]

3.3. Electric field-dependent conductivity for CNT-introduced ZnO matrix

In order to improve the quantum tunneling effect in the conductive mechanisms in CNT-introduced composite material, the CNT-matrix potential barrier were to be lowered. In the experiments, the insulating matrix was substituted to be the ZnO semiconductor. ZnO is an traditional semiconductor material, it has important and promising applications in the electronics technology.[20, 21, 22] Fig. 3 shows the XRD patterns of ZnO sample and CNT-introduced ZnO sample formed in the sol-gel processes. The XRD patterns were all indexed to the typical hexagonal wurtzite phase of ZnO, indicating that the introduction of CNTs has not affected the lattice structure of ZnO. Based on the XRD data and Scherrer's equation, the size of CNT-introduced ZnO monocrystal in CNT-introduced ZnO sample can be determined to be in nanometer magnitude. However, the scanning electron microscopy data indicated that the sizes of CNT-introduced ZnO sample were in micrometer magnitude. Consequently, it can be determined that the as formed CNT-introduced ZnO sample has a polycrystalline structure.

In contrast to the CNT-introduced insulating matrix, the conductive performance of CNT-introduced ZnO matrix is distinctive because its conductivity (or resistivity) is not only dependent of the CNT content, but also dependent of the applied electric field when the CNT content is in a certain range. As shown in Fig. 4, when the CNT content in multi-walled CNT-introduced ZnO matrix is far below the electric percolation threshold ($P_{th} \approx 1.5\%$), the electric field dependence of the resistivity may be neglected, the CNT-introduced ZnO matrix has a relatively higher resistivity which is independent of the applied electric field. However, for a CNT content approaching the electric percolation threshold P_{th}, the resistivity of CNT-introduced ZnO matrix is decreased and the decrease in resistivity becomes progressively drastic (dR/dE is enlarged) with the increasing of the applied electric field, until ultimately the resistivity tends to be a constant of a rather lower value (dR/dE decreases to 0). Meanwhile, for a higher CNT content near the electric percolation threshold, the resistivity of multi-walled CNT-introduced ZnO matrix is decreased more rapidly (dR/dE is larger) with the increasing of the applied electric field, and the variation range of electric field corresponding to the drastic decrease of resistivity is reduced. In addition, when the CNT content is further higher, a certain extently exceeding the electric percolation threshold, the resistivity of CNT-introduced ZnO matrix begins to be rather lower, reverting to be a constant independent of the applied electric field.

So far, the electric field-dependent conductivity for CNT-introduced ZnO matrix was identified to have been achieved owing to the distinctive performances, proper content of CNTs and the irreplaceable functions of semiconductor matrix.

3.4. Related mechanisms in the electric field-dependent conductivity for CNT-introduced ZnO matrix

In general, when a high electric field is applied, forming a negative electrical potential on a conductor surface, the electrons inside the conductor may penetrate the conductor-vacuum potential barrier, emitting out into the vacuum by the quantum tunneling effect.[23-26] As shown in Fig. 5, the electric field on the conductor surface is E_{local}; the work

function of the conductor is $\phi_0 = E_0 - E_F$, where E_0 is the vacuum level and E_F is the Femi level of the conductor. Taking into account the image potential relative to the conductor surface, the conductor-vacuum potential barrier may be formulated to be,

$$E_{barrier}(x) = \phi_0 - qE_{local} \cdot x - \frac{q^2}{16\pi\varepsilon_0 \cdot x} \qquad (0 < x < x_0) \tag{1}$$

The field emission current density can be quantitatively investigated by Fowler-Nordheim formula, which may be given in a simple and approximate form as follows,

$$J = \frac{1.56 \times 10^{-6} E_{local}^{\ 2}}{\phi} \cdot \exp\left(- \frac{6.83 \times 10^7 \phi^{\frac{3}{2}}}{E_{local}} \right) \tag{2}$$

Where ϕ is the height (maximum of $E_{barrier}(x)$) of the potential barrier.[24, 25] It can be seen in formula (2) that J would be larger when ϕ is lower and E_{local} is higher. It has been reported that to achieve a considerable field emission current density, the electric field on the conductor surface should be in the order of 10^7 V/cm. This is a rather higher electric field difficult to achieve.[25]

CNTs have diameters in nanometer magnitude and lengths in micrometer magnitude, possessing one-dimensional morphology of rather larger aspect ratios in the order of 10^3 and conductivity in the order of 10^4 S/m. The work function of CNT is 4.6eV. Owing to the unique structure, lower work function and excellent conductivity, CNT has distinctive field emission properties, which is originated in the remarkable field enhancement effect.[27-30] Under the stimulation of the applied macroscopic electric field E_{macro}, a much higher local electric field E_{local} would be initiated on the top of CNT. A field enhancement factor is involved, defined as,

$$\beta = \frac{E_{local}}{E_{macro}} \tag{3}$$

In general, β is the function of aspect ratio, the larger the aspect ratio, the higher the factor β. The previous research work indicated that β may be much higher (e.g., in the order of

10^3), as a result, the CNTs are capable of emitting a considerable current density up to 1A/cm^2 under a lower macroscopic electric field in the order of 10^4 V/cm.

In the CNT-introduced composite matrix, the orientations of CNTs should be distributed randomly and the configurations of the adjacent CNTs form noncoplanar lines predominantly. When the macroscopic electric field E_{macro} is applied in the matrix, the body electric potential is different for different positions in the direction of E_{macro}. However, owing to the high electrical conductivity of CNTs (~1.5×10^4 s/m), the space occupied by a CNT is an equipotential body in the matrix and the corresponding electric potential is a constant. The constant electric potential of a CNT should be equal to the body electric potential at the middle point of the CNT when the CNT is not presented in the matrix. As shown in Fig. 6, a and b stand for two adjacent CNTs with different orientations in the matrix, and oo' is their common perpendicular with length d, d may be seen to be the average distance of adjacent CNTs in the matrix. The middle points of a and b are A and B, respectively. The component of AB in the direction of E_{macro} is l. Consequently, the electric potential difference between a and b should be,

$$\Delta V_{ab} = E_{macro} \cdot l \tag{4}$$

The average electric field between these two adjacent CNTs (i.e., between o and o') should be,

$$\overline{E}_{oo'} = \frac{E_{macro} \cdot l}{d} \tag{5}$$

The local electric field E_{local} at the sidewalls of CNTs (o or o') may be much higher than $\overline{E}_{oo'}$, as indicated by the electric field lines in the illustration in Fig. 6, and this is originated in the thin sizes of CNTs. Consequently, a local field enhancement factor is involved, having the following relation,

$$E_{local} = \beta \cdot \overline{E}_{oo'} = \frac{\beta l}{d} \cdot E_{macro} \tag{6}$$

It is apparent that relative to the macroscopic electric field E_{macro}, the field enhancement factor for the two adjacent CNTs is $\frac{\beta l}{d}$.

According to solid state physics, a conductor-semiconductor contact structure is a Schottky junction with a certain potential barrier. Taking into account the image potential relative to the conductor surface, the conductor-semiconductor (n-type) potential barrier should be formulated to be,

$$E_{barrier}(x) = \phi_0 - x' - \frac{q^2 N_D}{\varepsilon_0 \varepsilon_r}\left(x_d x - \frac{1}{2}x^2\right) - \frac{q^2}{16\pi\varepsilon_0\varepsilon_r \cdot x} \quad (0 < x < x_0) \qquad (7)$$

Where ϕ_0 is the work function of the conductor, x' is the electron affinity of the semiconductor, N_D is the donator concentration in the semiconductor and x_d is the width of the potential barrier, as shown in Fig. 7. Owing to the presence of intrinsic defects, ZnO is a n-type semiconductor. The energy gap of ZnO is 3.37 eV and the electron affinity energy of ZnO is 2.1 eV.[20, 21] In the CNT-introduced ZnO matrix, in the view point of circuit interconnections in the microscope, there are two equivalent conductor-semiconductor contact structures with equivalent potential barriers being series connected between the adjacent CNTs with a tiny distance. In Fig. 6, the two conductor-semiconductor contact structures and their potential barriers are located at o on the sidewall of b and o' on the sidewall of a, respectively. However, when the macroscopic electric field is applied in the CNT-introduced ZnO matrix, the impedance characteristics of these two conductor-semiconductor contact structures should be different. In view of the direction of macroscopic electric field in Fig. 6, the contact structure at o' on the sidewall of a is under forward bias, while the contact structure at o on the sidewall of b is under reverse bias. As a result, a higher impedance is dominated for the conductor-semiconductor contact structure at o, largely determining the series impedance characteristic between the two adjacent CNTs.

For a Schottky junction under forward bias, such as the conductor-semiconductor (n-type) contact structure at o' on the sidewall of a, the impedance characteristic should accord with the diffusion theory or the thermionic emission theory. The alternative

applicability of these two theories lies in whether or not the mean free path of an electron in the semiconductor is larger than the width of the potential barrier.[19] However, for a Schottky junction under reverse bias, such as the conductor-semiconductor (n-type) contact structure at o on the sidewall of b, the impedance characteristic should accord with the field emission theory. Consequently, the impedance characteristic of the conductor-semiconductor contact structure under reverse bias should be able to be qualitatively investigated by Fowler-Nordheim formula. It should be noted that when the local electric fields are of the same, the conductor-semiconductor (n-type) potential barrier should be lower and narrower than the conductor-vacuum potential barrier due to the electron affinity energy of the semiconductor, while they should have the same characteristics in field emission.[19]

In the view point of statistics, when the CNT content is increased approaching the electric percolation threshold P_{th} in the CNT-introduced composite matrix, the average distance d between the adjacent CNTs is decreased, tending to 0 (i.e., the adjacent CNTs tend to contact each other). Consequently, the field enhancement factor $\frac{\beta l}{d}$ may be very large. In this case, the local electric field E_{local} on the sidewalls of CNTs (at o and o'), given in formula (6), would increase swiftly with the increasing of E_{macro}. Owing to the increase of E_{local} at o, the field emission current of the conductor-semiconductor contact structure (under reverse bias) at o on the sidewall of b would increase. Based on Fowler-Nordheim formula, the derivative of field emission current density may be given to be,

$$\frac{dJ}{dE_{local}} = \frac{1.56\times10^{-6}}{\phi}\cdot\left(2E_{local}+6.83\times10^{7}\phi^{\frac{3}{2}}\right)\cdot\exp\left(-\frac{6.83\times10^{7}\phi^{\frac{3}{2}}}{E_{local}}\right) \quad (8)$$

It can be seen in formula (8) that the field emission current at o, i.e., the current between the adjacent CNTs should increase super-linearly (increasing of J becomes progressively drastic) with the increasing of E_{local}. Herein, it should be noted that the super-linear increase of J means the tunneling impedance at o on the sidewall of b is not a

constant, it is decreased with the increasing of E_{local}. On the other hand, the relatively lower impedance of the conductor-semiconductor contact structure (under forward bias) at o' on the sidewall of a is simultaneously decreased owing to the increase of E_{local} at o'. It can be expected that when the applied macroscopic electric field E_{macro} is high, leading to a rather higher E_{local}, then the impedance between a and b, i.e., the series impedance of the two conductor-semiconductor contact structures between the adjacent CNTs, should be substantially decreased.

So far, the related mechanisms in the electric field-dependent conductivity for CNT-introduced ZnO matrix may be clarified. In essence, the electric field-dependent conductivity for CNT-introduced ZnO matrix is a macroscopic quantum tunneling effect. The CNT-introduced ZnO matrix with CNT content approaching the electric percolation threshold may be seen to be a three-dimensional disconnected network of CNTs interacting with a semiconductor matrix. The CNTs with excellent electrical conductivity and large aspect ratios act as conductive channels and the close areas of adjacent CNTs in the matrix are equivalent to electric field-dependent impedances. In fact, there must be a large amount of adjacent CNTs being contacted or apart from each other in the matrix, in these cases the impedances between the adjacent CNTs should be seen to be infinitesimal and infinite, respectively. The CNT-introduced ZnO matrix may be treated to be a comprehensive circuit composed of a large amount of electrical field-dependent impedances being series and parallel connected. With the increasing of the applied macroscopic electric field in the CNT-introduced ZnO matrix, these impedances would be decreased, leading to the inevitable decrease in resistivity of the CNT-introduced matrix. Meanwhile, the higher the CNT content (around the electric percolation threshold) in the matrix, the smaller the average distance between the adjacent CNTs, and the larger the field enhancement factor. As a result, the range of electric field corresponding to the resistivity decreasing of CNT-introduced ZnO matrix is reduced, as indicated in the experiments. In addition, with respect to the praparation of CNT-introduced ZnO matrix, the sufficient dispersibilities of multi-walled CNTs in ZnO matrix and the sufficient combination between multi-walled

CNTs and ZnO matrix should be the prerequisites for the stable and distinctive performances of CNT-introduced ZnO matrix.

4. Conclusion

The electric field-dependent conductivity was achieved for the multi-walled CNT-introduced ZnO matrix with CNT content approaching the electrical percolation threshold. The CNT-introduced ZnO matrix may be seen to be a three-dimensional disconnected network of CNTs interacting with a semiconductor matrix. In the view point of circuit interconnections in the microscope, there are two conductor-semiconductor contact structures being series connected between the adjacent CNTs, and the corresponding impedance between the adjacent CNTs is decreased with the increasing of the applied electric field. The CNT-introduced ZnO matrix may be treated to be a comprehensive circuit composed of a large amount of electrical field-dependent impedances being series and parallel connected. With the increasing of the applied macroscopic electric field in the CNT-introduced ZnO matrix, these series and parallel connected impedances would be decreased, leading to the inevitable decrease in resistivity of the CNT-introduced matrix.

Acknowledgements

This work was supported by Program of Educational Department in Heilongjiang Province of China (No. 12543070). We thank XiaoHua Tian and Qian Cheng (School of Materials Science and Engineering, Harbin Institute of Technology) for their warm-hearted help in the experiments.

References

1 Linxiang He, Sie Chin Tjong, *Nanoscale Research Letters.* 2013, **8**, 132.

2 Chun Yu Shang, Hui Kang, Hong Bo Jiang, Shu Po Bu, Xiao Hong Shang, *Journal of Luminescence*. 2013, **138**, 182.

3 Yangyang Zhang, Jinping Zhang, Jingxia Gao, Erping Wang, Hui Li, *J Mater Sci: Mater Electron*. 2013, **24**, 4170.

4 Q. Q. Yang, J. Z. Liang, *Appl. Phys. Lett*. 2008, **93**, 131918.

5 Yichuan Zhang, Huan Pang, Kun Dai, Yanfei Huang, Penggang Ren, Chen Chen, Zhongming Li, *J Mater Sci*. 2012, **47**, 3713.

6 Zijian Xu, Wei Zhang, Zhiyuan Zhu, Cuilan Ren, Yong Li, Ping Huai, *J. Appl. Phys*. 2009, **106**, 043501.

7 Kiran Jeet, V. K. Jindal, L. M. Bharadwaj, D. K. Avasthi, Keya Dharamvir, *J. Appl. Phys*. 2010, **108**, 034302.

8 Ji Hoon Lee, Man Tea Kim, Kyong Yop Rhee, Soo Jin Park, *Res Chem Intermed*. 2014, **40**, 2487.

9 Chunyu Shang, Xiuqin Wang, Ziyong Cheng, Zhiyao Hou, Jun Lin, *J. Appl. Phys*. 2013, **113**, 093101.

10 DaoQiang, Daniel Lu, Yi Grace Li, C. P.Wong, *Journal of Adhesion Science and Technology*. 2008, **22**, 815.

11 Xiaohong Shang, Deming Han, Dongfeng Li, Zhijian Wu, *Chemical Physics Letters*. 2013, **565**, 12.

12 Jin Young Kim, Duk Young Jeon, Hong Gun Yang, *Journal of The Electrochemical Society*. 2000, **147**, 3559.

13 S. R. Sivakkumar, A. G. Pandolfo, *J Appl Electrochem*. 2014, **44**, 105.

14 S. Pfeifer, S.H. Park, P. R. Bandarua, *J. Appl. Phys*. 2010, **108**, 024305.

15 Chunsheng Lu, Yiuwing Mai, *J Mater Sci*. 2008, **43**, 6012.

16 A. Bid, A. Bora, A. K. Ryachaudhuri, *Phys. Rev. B*. 2006, **74**, 035426.

17 S. Maitrejean, T. Mourier, A. Toffoli, G. Passemard, *Microelectron. Eng*. 2006, **83**, 2396.

18 Sun Y, Bao H D, Guo Z X, Yu J, *Macromolecules*. 2009, **42**, 459.

19 E. K. Liu, B. S. Zhu, J. S. Luo, *Semiconductor Physics* [M]. National Defense Industry Publishers, Beijing (1994).

20 EunHa Shin, Hanchul Kim, *Journal of the Korean Physical Society*. 2014, **64**, 543.

21 Wei Li, Dongsheng Mao, Fumin Zhang, Xi Wang, Xianghuai Liu, Shichang Zou, *J. Vac. Sci. Technol. B*. 2001, **19**, 3.

22 Xiaohong Shang, Deming Han, Shuang Guan, Gang Zhang, *J. Phys. Org. Chem*. 2013,

26, 784.

23 J. X. Fang, L. Dong, *Solid State Physics* [M]. Shanghai Scientific and Technical Publishers, Shanghai (1981).

24 J. Plsek, D. Zhukov, Z. Knor, *Journal of Physics*. 2002, **52**, No. 12.

25 T. Ouisse, *Eur. Phys. J. B*. 2001, **22**, 415.

26 Xiaohong Shang, Yuqi Liu, Xiaochun Qu, Zhijian Wu, *Journal of Luminescence*. 2013, **143**, 402.

27 D. Lei, L. Y. Zeng, W. B. Wang, *J. Appl. Phys*. 2007, **102**, 114503.

28 S. C. Ray, U. Palnitkar, C. W. Pao, H. M. Tsai, W. F. Pong *et al, J. Appl. Phys*. 2008, **104**, 063710.

29 Preeti Verma, Prashant Kumar; Seema Gautam, Poornendu Chaturvedi *et al, Fullerenes, Nanotubes and Carbon Nanostructures*. 2009, **17**, 249–257.

30 J.M. Bonard, J.P. Salvetat, T. Stöckli, L. Forr´o, A. Châtelain, *Appl. Phys. A*. 1999, **69**, 245–254.

Figures:

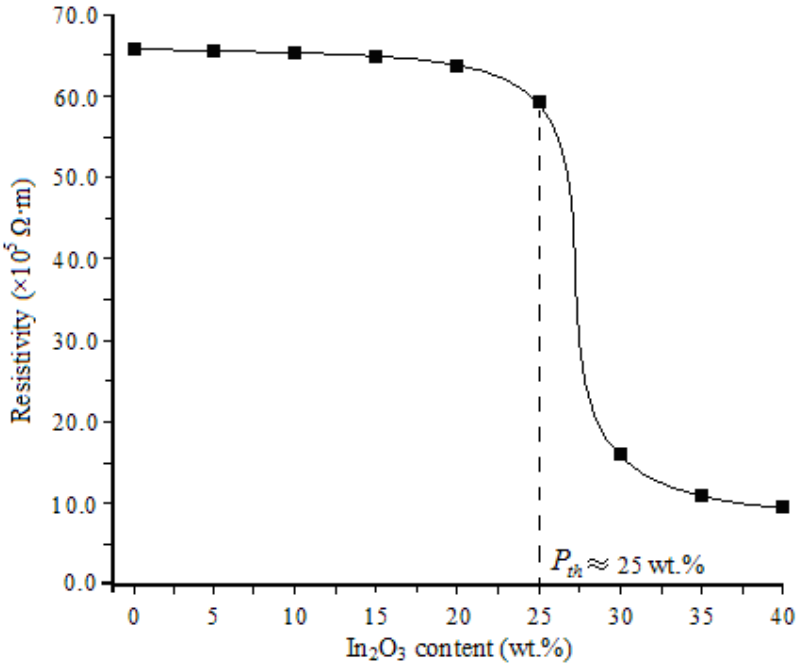

Fig. 1 Resistivity-In_2O_3 content relation for In_2O_3-introduced Y_2O_3 matrix.

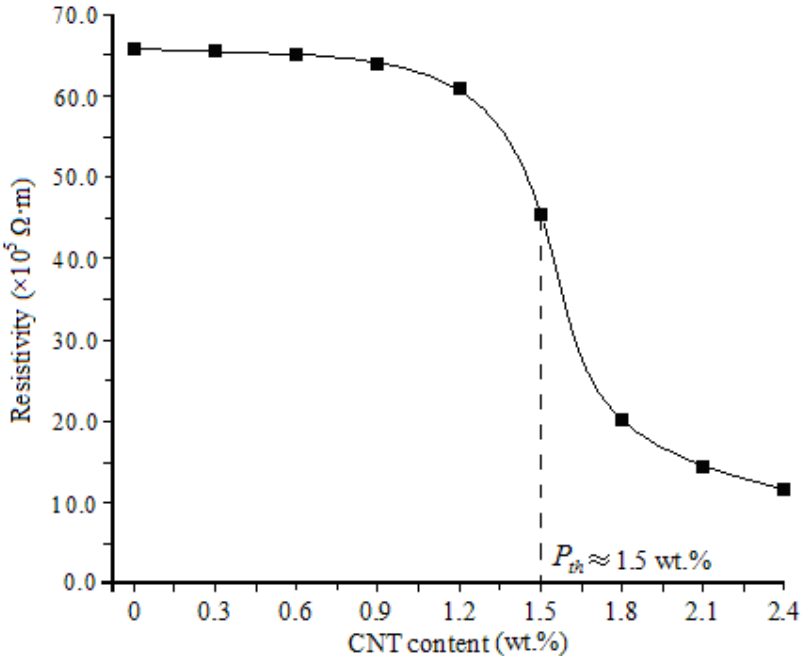

Fig. 2 Resistivity-CNT content relation for multi-walled CNT-introduced Y_2O_3 matrix.

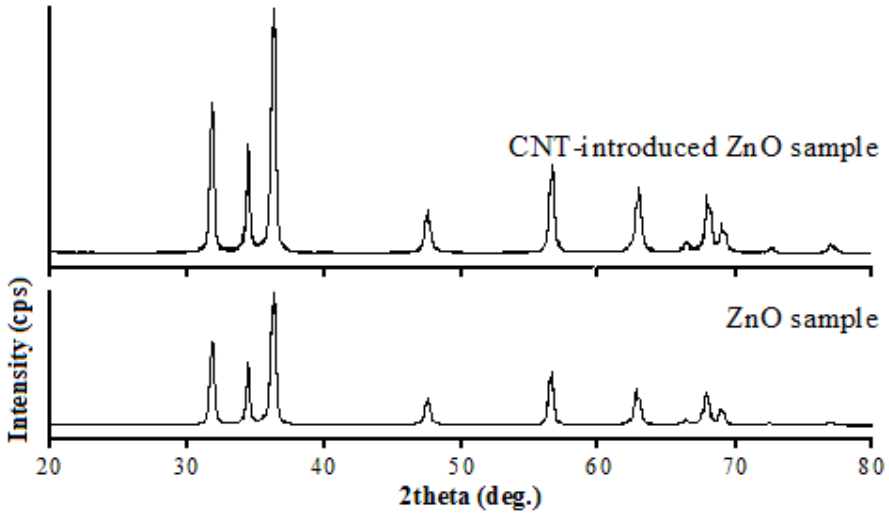

Fig. 3 XRD patterns of ZnO sample and CNT-introduced ZnO sample formed in the sol-gel processes.

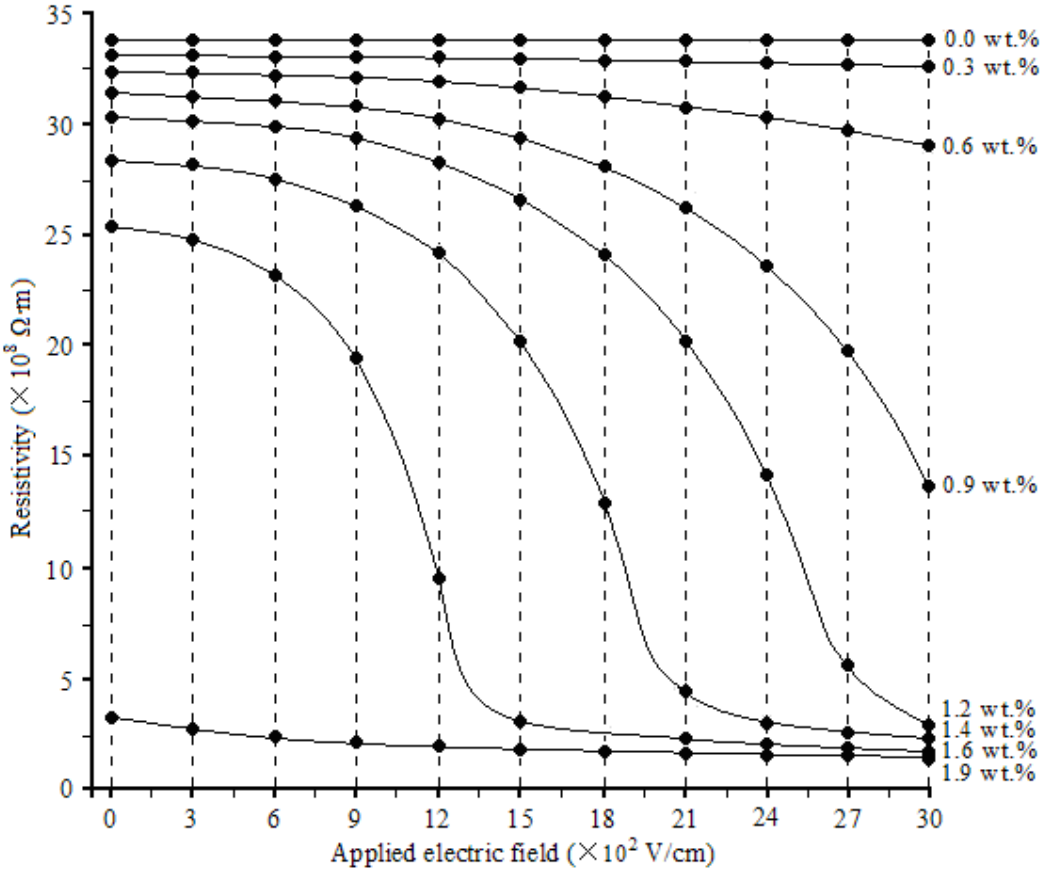

Fig. 4 Electric field-resistivity relations for different CNT contents in multi-walled CNT-introduced ZnO matrix.

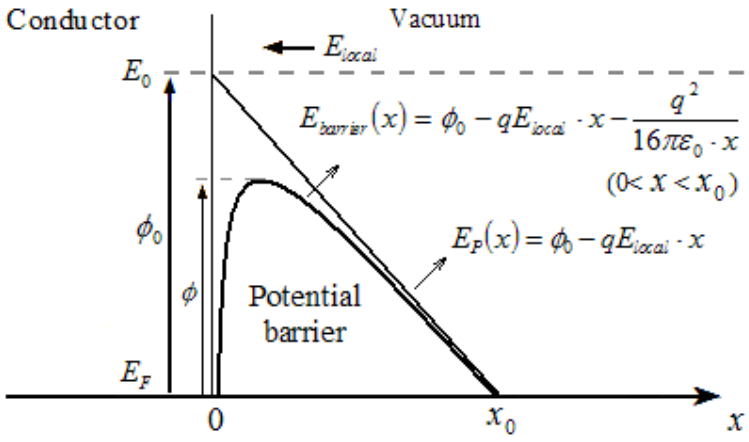

Fig. 5 Conductor-vacuum potential barrier in the local electric field.

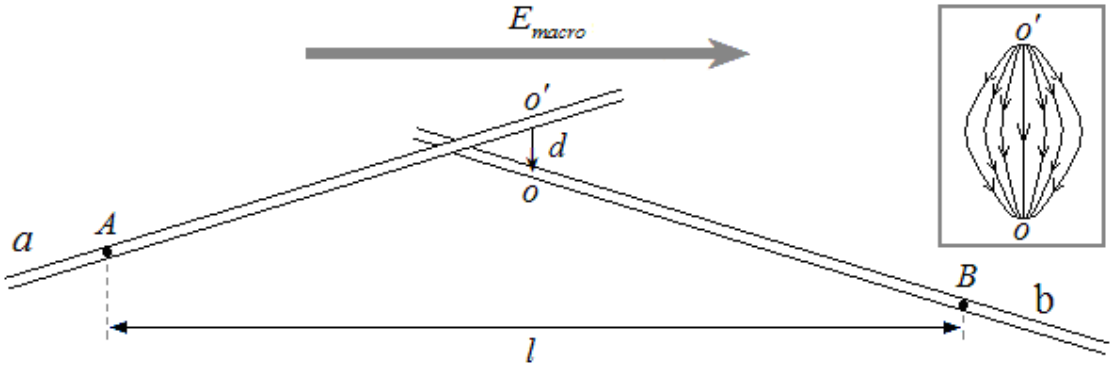

Fig. 6 Two adjacent CNTs in the applied macroscopic electric field, the illustration shows the electric field lines between the adjacent CNTs.

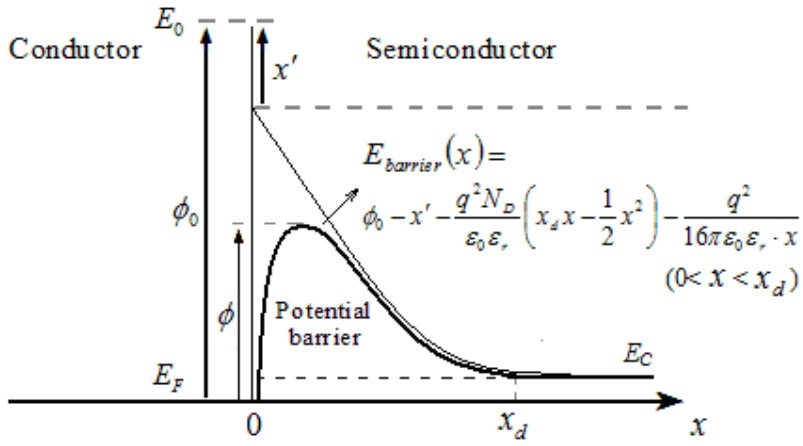

Fig. 7 Potential barrier of conductor-semiconductor (n-type) contact structure in the equilibrium state.